RESEARCH ARTICLE

Do the Ni binding modes on $C_{12}N_{12}$ cluster influence its H_2 trapping capability?

Gourhari Jana[1], Ranita Pal[1], Sukanta Mondal[2,*], Pratim Kumar Chattaraj[1,3,*]

[1]Department of Chemistry and Center for Theoretical Studies, Indian Institute of Technology Kharagpur, 721302, India
[2]Department of Education, A M School of Educational Sciences, Assam University, Silchar, Assam 788011, India
[3]Department of Chemistry, Indian Institute of Technology Bombay, Mumbai 400076, India

*Corresponding authors: E-mail: sukanta.mondal@aus.ac.in; sukanta.mail13@gmail.com; pkc@chem.iitkgp.ac.in

DOI: 10.5185/amlett.2020.041500

In order to introduce a new promising material for hydrogen storage application, Nickel (Ni) has been decorated on $C_{12}N_{12}$ nano-cluster. Firstly, the binding mode of Ni on $C_{12}N_{12}$ could be thought to be a bridge in between C, N (denoted as C-(μ-Ni)-N) or C, C (denoted as C-(μ-Ni)-C) or N, N (denoted as N-(μ-Ni)-N) resulting in three distinct geometries (abbreviated as X_{CN}, X_{CC}, and X_{NN} isomers, respectively). Owing to the variation in the bridging mode of Ni, the interacting properties with the hydrogen molecule are expected to be different. The spontaneity of formation of Ni-$C_{12}N_{12}$ and 4Ni-$C_{12}N_{12}$ in terms of ΔH^{o}_{f} of isodesmic reactions indicate the possibility of getting promising high-energy-density materials (HEDMs). Further, we have investigated whether Ni, being a 3d transition metal, can influence the aromatic behavior of $C_{12}N_{12}$ nano-cluster. The binding energies and natural bond orbital (NBO) charges have been computed and energy decomposition analysis is carried out for Ni-$C_{12}N_{12}$ isomers. Decoration of Ni on X_{CN} isomer releases slightly lower energy (~107.4 kcal/mol versus ~58.6 kcal/mol for X_{NN} and X_{CN} respectively). The hydrogen adsorption capacity of the strongest and the weakest Ni-bonded Ni-$C_{12}N_{12}$ nano-clusters (X_{NN} and X_{CN} isomers, respectively) has also been investigated.

Introduction

The growth in population and the ever-increasing demand for urbanization is resulting in the depletion of fossil energy sources. The exploitation of fossil fuels is having numerous adverse effects on the planet and its environment since burning hydrocarbon deposits like oil, coal, etc. release carbon dioxide which is one of the main culprits in causing global warming. Currently, energy supply for running automobiles, power plants, household furnaces, etc. are mainly provided by burning fossil fuels. Hence it is high time for the scientific community to look for alternative eco-friendly energy sources. To that end, Hydrogen is turned out to be a clean and effective fuel owing to properties like lightweight, abundance in nature, recyclability, renewability, its combustion producing zero pollution, etc. [**1-4**] For example, a fuel-cell automobile running on hydrogen fuel will travel more distance than one running on an equal amount of gasoline. Despite such benefits, incorporating hydrogen as the major energy carrier into the world economy becomes challenging due to the high storage cost and limited large-scale transportation. Consequently, there has been a rise in interest and investments toward research and development on high capacity hydrogen storage materials. Desirable characteristics for suitable and efficient hydrogen storage materials include high volumetric and gravimetric densities, fast adsorption and desorption kinetics at ambient conditions, favorable enthalpies, recyclability, safety, and cost-effectiveness [**5-7**]. Several options are being extensively explored on that front, such as carbon-based materials (activated carbons, carbon nanotubes, nanofibers, fullerenes, templated porous carbons, etc.) [**8-12**], porous polymers [**13**], clathrate hydrates [**14,15**], zeolites [**16-19**], alumina, silica [**20-23**], metal-organic frameworks (MOFs) [**24,25**], covalent organic frameworks (COFs) [**26,27**], aerogels [**28,29**], alanates [**30**], boron nitride materials [**31**], Lithium-phosphorus double helix [**32**] and metal borohydrides [**33**]. Although research work is going on in all possible branches with the target of achieving hydrogen fuel as one of our reliable energy resources, we are yet to achieve hydrogen powered automobiles and instruments in a cost-effective manner. This failure stimulates the strong effort towards reaching the target for hydrogen storage established by bodies like DOE.

Hydrogen interaction with transition metals is very important in numerous chemical processes and fundamental aspect of many key reactions in different applications of chemical industries, especially when it comes to H_2 storage and its purification [**34,35**]. Approaches made on hydrogen-storage by metal hydrides [**36**], different metal complexes and nanoparticles [**37-41**] including those of Fe [**42**], Ru [**43**], Ni [**44-46**], Pt [**47**], Pd [**48**] have been extensively studied and reported. Comprehensive studies performed by Ferrin *et al*. [**49**], Yarovsky *et al*. [**50**], and Jagiello *et al*. [**51**] on interaction

of hydrogen with seventeen different transition metals, on Al_{13} cluster, and porous carbons, respectively, have been very impactful in understanding the adsorption potential of hydrogen.

AlN nano-cages (spherical) and nanostructures have been found to be sufficiently capable of storing hydrogen, as reported by Guo *et al*. [**52**] and Wang *et al*. [**53**] respectively. In the recent past, theoreticians have reported some metal-doped and decorated nanostructures [**54-59**] along with their pure analogues for hydrogen storing purposes. Khurshid and his co-worker have carried out nickel adsorption on the surface of $Al_{12}P_{12}$ [**60**] and found four possible sites for nickel atom decoration. Furthermore, it was found that transition metal atom doping in nano-clusters, particularly Ti, V, Ni, and Pd were extensively used to increase the hydrogen storage potential of clusters [**61**] and also in the hydrogenation reaction.

In 2011, Chattaraj *et al.* have studied the hydrogen adsorption ability of $B_{12}N_{12}$ cluster [**62**]. Later on, Wen-Jie *et al*. in 2012 have investigated the hydrogen storage behavior of the Li-decorated $B_{12}N_{12}$ cluster using density functional theory [**63**]. Rad *et al*. have examined the hydrogen adsorption on Ni-decorated $B_{12}N_{12}$ nano-cages [**64**]. Carbon-based nanostructures are too inert to be used in most of the technological applications unless they are functionalized with heteroatoms. The existence of cyanogens nanocluster ($C_{12}N_{12}$), has been verified in many theoretical as well as experimental studies [**65-68**]. In line with our research group's quest, recently, the hydrogen storage efficacy and stability of this nanocluster has been investigated by Chattaraj *et al*. [**69**] Now, the approach is being taken here to investigate the hydrogen storage potential of exohedrally doped, Ni atom(s) decorated $C_{12}N_{12}$ nanocluster which is quite natural and interesting. Out of the three ways of bridging modes of Ni, N-(μ-Ni)-N mode of binding (X_{NN}), is found to be stronger than that in C-(μ-Ni)-N (X_{CN}) and C-(μ-Ni)-C (X_{CC}) reflected by the adsorption energy and the free energy change of adsorption. The polar nature of Ni-CN or Ni-NN bond and positive charge on Ni center can polarize and thereby interact and adsorb hydrogen (H_2) molecules, thus resulting in efficient storage for molecular hydrogen.

Aromaticity is one of the well-known topics in chemistry by which one can fetch crucial information of a system [**70**]. Quantum mechanical approach helped in understanding and characterizing the aromaticity and stability of simple compounds with the Hückel's (4n+2) π-electron rule [**71-73**]. The aromatic stabilization was then extended to heterocyclic compounds [**74,75**] and inorganic compounds, including metal clusters [**71,72,76-89**]. The impact of aromaticity on the geometrical and electronic structure, reactivity and magnetic properties of many molecular moieties helps us to observe it in an indirect manner. Due to the virtual and imprecise nature of aromaticity, numerous attempts have been developed to find out appropriate descriptors and indices like resonance energy (RE) [**90**], aromatic stabilization energy (ASE) [**91**], isomerization stabilization energy (ISE) [**92**], Julg index [**93,94**], harmonic-oscillator model of aromaticity (HOMA) [**88**] based on the equalization of bond lengths within the rings [**95**] Jug index [**96**], para-delocalization index (PDI) [**97**], Bird index [**98-100**], I_{ring} [**101,102**], aromatic fluctuation index (FLU) [**71,72**], FLU_{π}, electron density at the ring critical point (ρ_{RCP}) [**103,104**] bond order index of aromaticity (BOIA), multicenter delocalization index (MCDI) [**75,105**], para-linear response (PLR) [**106**], aromatic ring current shielding (ARCS) [**107**], ring current density plots (RCDP) [**108**], anisotropy of induced current density (AICD) [**109**], nucleus independent chemical shift (NICS) [**78,110**], $NICS_{zz}$, and NICS-XY-scan [**103,104,109,111**]. Among these, NICS is one of the simplest and most widely accepted descriptors. Several studies performed by Schleyer *et al.* [**112**], Ruiz-Morales [**113**], Robinson [**114, 115**] on polybenzoid hydrocarbons, polycyclic aromatic hydrocarbons (PAHs) and Ga_3^{2-} ring, respectively, have been reported which used NICS descriptor for characterization of aromaticity. In the following years, aromatic studies on clusters like Zintl, P_4 cluster have been performed by computing NICS [**116**].

In the present study, we have studied the aromatic behavior of Ni-decorated $C_{12}N_{12}$ cluster and the gradual increase in aromaticity with an increase in the number of Ni atoms exohedrally surrounded in N-(μ-Ni)-N mode of bridging by calculating NICS(0) values.

Computational details

The geometry optimization and subsequent frequency analysis of all the systems have been carried out using the ωB97X-D functional developed by Chai and Head-Gordon [**117**], which uses a version of Grimme's D2 dispersion model [118] and is reported to be suitable in representing non-covalent interactions. In conjunction, due to the presence of transition metal (Ni) in our studied system, Def2-TZVP basis set [**119,120**] is used. The real values of all frequencies ensure the existence of all the systems under investigation at the minima on the respective potential energy surfaces (PES). To calculate average adsorption energies (E_{ads}), and free energy change (ΔG_{ads}) per H_2 molecule the following expressions have been used:

$$E_{ads} = \frac{1}{n}\{E_{nH_2\cdots\text{systems}} - (E_{systems} + nE_{H_2})\}$$

$$\Delta G_{ads} = \frac{1}{n}\{G_{nH_2\cdots\text{systems}} - (G_{systems} + nG_{H_2})\}$$

All these computations are done using Gaussian 09 program package [**121**].

The natural population analysis (NPA) [**122,123**] scheme is adopted to compute atomic charges (QNPA).

Energy decomposition analysis (EDA) was carried out at the revPBE-D3 [**124,125**]/TZ2P//ωB97X-D/Def 2-TZVP level using ADF 2013.01 program package [**126, 127**] and the scalar relativistic effects are considered for the heavy elements using the zeroth-order regular

approximation (ZORA) [**128**]. The total interaction energy (ΔE_{int}) between two fragments in EDA can be represented as the summation of three attractive energy terms, *viz*., the electrostatic interaction energy (ΔV_{elstat}), orbital interaction energy (ΔE_{orb}), dispersion interaction energy (ΔE_{disp}, and one repulsive energy term, namely, Pauli repulsion energy (ΔE_{Pauli}).

Therefore, ΔE_{int} can be written as,

$$\Delta E_{int} = \Delta E_{Pauli} + \Delta V_{elstat} + \Delta E_{orb} + \Delta E_{disp}$$

In order to calculate NICS, a ghost or dummy atom (Bq) is considered at the geometric center of the Ni-$C_{12}N_{12}$ cages (denoted by NICS(0)). A normal NMR calculation suggests the chemical shifts for all atoms, including the ghost atom under consideration. According to NICS definition, we have reported the $NICS_{iso}$ values as negative on multiplying by -1. The negative NICS indices suggest the molecular system(s) is/are aromatic while positive value(s) suggest anti-aromatic character of the system(s). NMR shielding tensors are computed in G09 program with the Gauge-Independent Atomic Orbital (GIAO) method in ppm unit. NICS(0) is considered as a gauge of the σ+π-electron delocalization.

Results and discussion

Structure, stability and reactivity

We have taken cyanogen clathrates which are made up of CN linkages encircling twelve units to form $C_{12}N_{12}$ nano-clusters. Out of the three reported isomers [**69**], the most symmetric isomer is considered here for Ni decoration and H_2 storage purposes since it is reported to be capable of possessing maximum H_2 adsorption capacity. In the present study, we have investigated the stability of Ni-decorated $C_{12}N_{12}$ clusters with different possible bridging modes of Ni *viz*. N-(μ-Ni)-N, C-(μ-Ni)-C and C-(μ-Ni)-N which are abbreviated as X_{NN}, X_{CC}, and X_{CN}, respectively. The optimized geometries of all the studied clusters are depicted in **Fig. 1** and **Fig. 2**. The binding energy (E_b, kcal/mol), free energy change (ΔG_b, kcal/mol) for the formation of Ni-decorated $C_{12}N_{12}$ clusters along with the natural charge at Ni center (q_{Ni}, $|e|$), and the energy gap ($\Delta E_{H\text{-}L}$, eV) between highest occupied molecular orbital (HOMO) and the lowest unoccupied molecular orbital (LUMO) computed at ωB97X-D/Def2-TZVP level are provided in **Table 1**. It is clear from **Table 1** that the binding energy of Ni with $C_{12}N_{12}$ cluster in X_{NN} isomer is higher than those of the other two modes, namely, X_{CC} and X_{CN} (least one). So, we have extended the doping process in X_{NN} isomer up to a maximum of four Ni atoms (see **Fig. 2**). Further, the change in the HOMO-LUMO energy gap (ΔE_{H-L}, eV) on Ni bound clusters is investigated in order to observe the change in reactivity since ΔE_{H-L} is often used as a reactivity indicator. Due to Ni binding, the ΔE_{H-L} decreases and it reaches the lowest in the case of X_{CN} isomer and the highest for X_{CC} suggesting the highest reactivity in case of C-(μ-Ni)-N bridging mode. The natural charge on the Ni center in X_{CN}, X_{CC}, and X_{NN} isomers vary within 0.53−0.81|e| where Ni in X_{NN} isomer acquires the highest positive charge (due to the coordination of two more electronegative N atoms) indicating that this isomer can be used as the best potential material for hydrogen storage purpose. The natural charge on the Ni center in both of the X_{CN} and X_{CC} isomers are the same and they attain the least value. On decorating more Ni atoms *i.e*., maximum up to four, the natural charge on Ni gradually decreases as observed from **Table 1**, and reactivity also increases which is reflected in ΔE_{H-L}, accordingly.

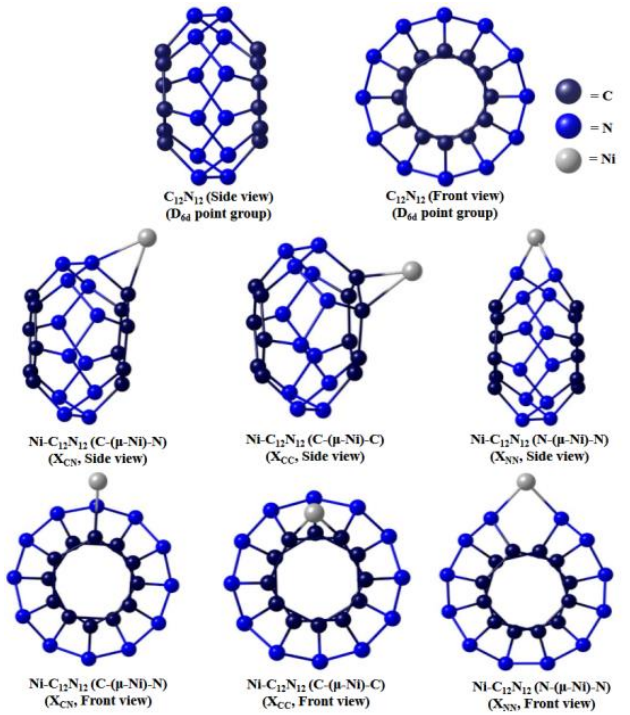

Fig. 1. Optimized structures of Ni bound $C_{12}N_{12}$ cluster in different bridging modes (Side view and Front view) computed at the ωB97X-D/Def2-TZVP level.

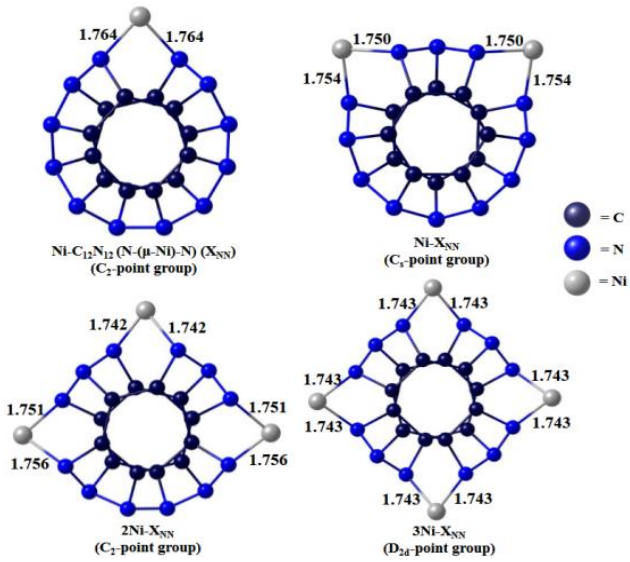

Fig. 2. Optimized structures of nNi-decorated $C_{12}N_{12}$ clusters (n=1-4) at the ωB97X-D/Def2-TZVP level.

Table 1. The binding energy (E_b, kcal/mol), free energy change (ΔG_b, kcal/mol) (per Ni molecule), natural charge at Ni center (q_{Ni}, $|e|$), HOMO-LUMO energy gap ($\Delta E_{H\text{-}L}$, eV) at the ωB97X-D/Def2-TZVP level.

Systems	E_b per Ni	ΔG_b per Ni	q_{Ni}	$\Delta E_{H\text{-}L}$
$C_{12}N_{12}$				7.6
Ni-$C_{12}N_{12}$ (X_{CN})	-58.6	-50.7	0.53	6.0
Ni-$C_{12}N_{12}$ (X_{CC})	-79.6	-71.0	0.53	7.1
Ni-$C_{12}N_{12}$ (X_{NN})	-107.4	-98.1	0.81	6.7
2Ni-$C_{12}N_{12}$ (Ni-X_{NN})	-102.3	-93.1	0.80	6.7
3Ni-$C_{12}N_{12}$ (2Ni-X_{NN})	-101.0	-91.9	0.78-0.79	6.5
4Ni-$C_{12}N_{12}$ (3Ni-X_{NN})	-96.8	-87.8	0.77	6.4

In order to prepare Ni decorated $C_{12}N_{12}$ clusters, we must study the thermodynamics of their formation, which we have carried out in terms of isodesmic reaction. The dependence of their aromatic behavior on the extent of Ni doping on $C_{12}N_{12}$ cluster is also investigated by evaluating their corresponding NICS(0) values.

A) *Isodesmic reaction*

To analyze the spontaneity of formation of Ni-$C_{12}N_{12}$ (X_{NN}) and 4Ni-$C_{12}N_{12}$ (3Ni-X_{NN}), the heat of formation (ΔH^o_f) of isodesmic reactions are useful. Heat of formation (ΔH^o_f) of Ni-$C_{12}N_{12}$ and 4Ni-$C_{12}N_{12}$ are first calculated using theoretically computed enthalpies of Ni-$C_{12}N_{12}$, C, N, Ni and 4Ni-$C_{12}N_{12}$ at ωB97X-D/Def2-TZVP level of theory:

$$\Delta H^{\circ}_{f\,(Ni\text{-}C_{12}N_{12})} = H_{(Ni\text{-}C_{12}N_{12})} - \{12H_C + 12H_N + H_{Ni}\}$$

$$\Delta H^{\circ}_{f\,(4Ni\text{-}C_{12}N_{12})} = H_{(4Ni\text{-}C_{12}N_{12})} - \{12H_C + 12H_N + 4H_{Ni}\}$$

$\Delta H^{\circ}_{f\,(Ni\text{-}C_{12}N_{12})}$ and $\Delta H^{\circ}_{f\,(4Ni\text{-}C_{12}N_{12})}$ are then used along with experimental ΔH^o_f values of ethylene, ammonia, hydrazine, nickel, and pyrrole [**129,130**] to calculate the ΔH^o_f of the following isodesmic reactions.

Ni-$C_{12}N_{12}$ + 12H_2C=CH_2 + 3NH_3 —› 9C_4H_4NH + 3H_2N–NH_2 + Ni

4Ni-$C_{12}N_{12}$ + 12H_2C=CH_2 + 3NH_3 —› 9C_4H_4NH + 3H_2N–NH_2 + 4Ni

Calculated ΔH^o_f values are 4239.470 and 4520.528 kcal/mol for Ni-$C_{12}N_{12}$ and 4Ni-$C_{12}N_{12}$ isomers, respectively, suggesting the formation of the latter to be slightly more spontaneous.

B) Aromaticity of Ni-$C_{12}N_{12}$ cluster

NMR analysis of the bare $C_{12}N_{12}$ cluster and Ni-decorated cluster have been done to describe aromatic stability by measuring NICS(0) values. A negative NICS(0) value for the bare $C_{12}N_{12}$ cluster supports the existence of its aromatic behavior. The decoration of Ni atom(s), maximum up to four, brings a significant change in the aromaticity. The NICS(0) value of $C_{12}N_{12}$ cluster is -3.937 ppm computed at the center of the cage using ωB97X-D/Def2-TZVP level of theory. All the NICS(0) data are presented in **Table 2**. NICS(0) value in case of the different bridging modes of Ni is different. It shows maximum value in the case of X_{NN} isomer, almost three times of that in the bare $C_{12}N_{12}$ and minimum in case of X_{CN} isomer indicating the highest aromatic behavior of X_{NN} isomer compared to other two isomers (X_{CN} and X_{CC}). The aromatic stabilization increases almost four times than that of the bare $C_{12}N_{12}$ on a maximum of four Ni atoms decoration on the X_{NN} isomer.

Table 2. Nucleus Independent Chemical Shift (NICS(0), ppm) values computed at ωB97X-D/Def2-TZVP level.

Systems	NICS(0)
$C_{12}N_{12}$	-3.937
Ni-$C_{12}N_{12}$(X_{CN})	-4.578
Ni-$C_{12}N_{12}$(X_{CC})	-4.691
Ni-$C_{12}N_{12}$(X_{NN})	-11.536
2Ni-$C_{12}N_{12}$(Ni-X_{NN})	-12.095
3Ni-$C_{12}N_{12}$(2Ni-X_{NN})	-13.700
4Ni-$C_{12}N_{12}$(3Ni-X_{NN})	-14.852

Hydrogen storage capacity

Inspired by the Ni-decorated BN nano-cluster by a prior report [**64**] where Ni shows superior performance for H_2 storage, we have chosen the exohedral decoration of Ni ad-atoms on $C_{12}N_{12}$. Due to such molecular modeling, positive charges developed on Ni atoms make it suitable for H_2 trapping. The optimized geometries the H_2 adsorbed configurations are given in **Fig. 3**. In the free state, the H-H bond distance of the H_2 molecule is 0.744 Å. In case of the exohedral doping of single Ni atom in C-(μ-Ni)-N binding mode with $C_{12}N_{12}$ cluster, adsorbing up to three H_2 molecules, the corresponding H-H bond lengths range from 0.767 to 0.820 Å, while those for N-(μ-Ni)-N binding mode lies within 0.748-0.780 Å (see the Fig. 2).

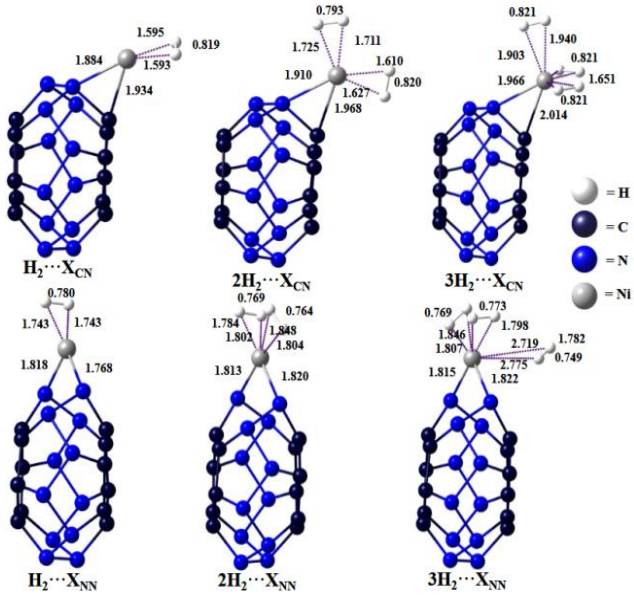

Fig. 3. Optimized structures of H_2 trapped single Ni bound $C_{12}N_{12}$ cluster at the ωB97X-D/Def2-TZVP level.

Table 3. The adsorption energy (E_{ads}, kcal/mol), adsorption free energy change (ΔG_{ads}, kcal/mol) (per H_2 molecule), natural charge at Ni center (q_{Ni}, $|e|$), HOMO-LUMO energy gap ($\Delta E_{H\text{-}L}$, eV) computed at the ωB97X-D/Def2-TZVP level.

Systems	E_{ads} per H_2	ΔG_{ads} per H_2	q_{Ni}	$\Delta E_{H\text{-}L}$
$H_2\cdots X_{CN}$	-23.3	-13.1	0.27	6.2
$2H_2\cdots X_{CN}$	-15.4	-5.2	0.12	6.2
$3H_2\cdots X_{CN}$	-11.9	-1.7	-0.21	6.2
$H_2\cdots X_{NN}$	-39.2	-28.9	0.62	6.6
$2H_2\cdots X_{NN}$	-22.9	-13.0	0.46	6.9
$3H_2\cdots X_{NN}$	-16.0	-6.6	0.44	6.9
$H_2\cdots$3Ni-X_{NN}	-11.4	-1.7		
$4H_2\cdots$3Ni-X_{NN}	-11.4	-1.4	0.56	6.1
$8H_2\cdots$3Ni-X_{NN}	-8.1	1.6	0.41	6.4

The adsorption energy (E_{ads}, kcal/mol), adsorption free energy change (ΔG_{ads}, kcal/mol) per H_2 molecule, natural charge at Ni center (q_{Ni}, $|e|$), and HOMO-LUMO energy gap ($\Delta E_{H\text{-}L}$, eV) of adsorbed H_2 are provided in **Table 3** computed using the same level of theory. We have computed the hydrogen adsorption energy and free energy per H_2 for the lowest and highest binding cases, *i.e*, X_{CN} and X_{NN} isomers, respectively. In all the cases, the negative values of adsorption free energy suggest an exergonic nature or the spontaneity of the process at room temperature (298 K) except in the case of 3Ni-X_{NN} which is endergonic by 1.6 kcal/mol and would be feasible at lower temperatures. Owing to the highest positive natural charge on Ni center in X_{NN} isomers (0.81|e|), it will polarize the H_2 molecule(s) maximum and accordingly this isomer can be considered as the best candidate for potential hydrogen storage material. We have investigated the improvement in H_2 storing capability in four Ni-doped $C_{12}N_{12}$ clusters (see **Table 1** and **Fig. 4**).

The adsorption energies (E_{ads}) per H_2 molecule has been calculated as:

$$E_{ads} = \frac{1}{n}\left[E\left(nH_2 \cdots X_{CN/NN}\right) - \left\{E\left(X_{CN/NN}\right) + E(nH_2)\right\}\right]$$

$$E_{ads} = \frac{1}{n}\left[E(nH_2 \cdots 3X_{NN}) - \{E(3X_{NN}) + E(nH_2)\}\right]$$

Each Ni atom in 3Ni-X_{NN} isomer binds a maximum of two H_2 molecules with binding energy ranging from -8.1 to -11.4 kcal/mol. The natural charge on Ni atom gets lowered on gradual H_2 loading, suggesting the charge transfer from the Ni center(s) of the Ni-$C_{12}N_{12}$ nano-cluster to the anti-bonding orbital of H_2. Similarly, the decrease in E_{ads} and G_{ads} values with an increase in the loaded number of H_2 molecules is noted. The reactivity change on H_2 adsorption of Ni-$C_{12}N_{12}$ nano-clusters is reflected in their HOMO-LUMO energy gap ($\Delta E_{H-L,}$ eV). In our studied cases, X_{CN} isomer shows that the reactivity decreases on H_2 loading and remains almost the same as we load a maximum of up to three H_2 molecules. In case of X_{NN} the reactivity decreases as we load 2-3 H_2 molecules but for a single H_2 case, a slight increase is observed.

Energy decomposition analysis

Further, we have examined the interaction energy (ΔE_{int}) and the contribution of energy terms towards total interaction which are responsible for stabilizing the $H_2\cdots$Ni-$C_{12}N_{12}$ interaction. EDA is carried out considering H_2 molecule(s) as one fragment and the Ni-$C_{12}N_{12}$ cluster as another (see **Table 4**). It is evident from the energy values per H_2 molecule that the electrostatic and orbital interactions are the primary contributors to the interaction energy, the contribution from the former being 50.5−57.8% while that from the latter is 41.0−48.0% of the total attractive energy. On the other hand, the dispersion interaction is almost negligible (ca. 1.1−5.7% of the total attraction).

Table 4. EDA results of H_2 bound Ni-decorated Ni-$C_{12}N_{12}$ and 4Ni-$C_{12}N_{12}$ clusters at the revPBE-D3/TZ2P//ωB97X-D/Def2-TZVP. All energy values reported here are per H_2 in kcal/mol. The values in parentheses are percentage contribution toward the total attraction, $\Delta V_{elstat} + \Delta E_{orb} + \Delta E_{disp}$.

Systems	ΔE_{int}	ΔE_{Pauli}	ΔV_{elstat}	ΔE_{orb}	ΔE_{disp}
$H_2\cdots X_{CN}$	-24.9	59.8	-48.9(57.8)	-34.8(41.0)	-1.0(1.2)
$2H_2\cdots X_{CN}$	-15.7	62.4	-43.1(55.2)	-34.2(43.7)	-0.9(1.1)
$3H_2\cdots X_{CN}$	-13.6	69.9	-42.2(50.5)	-40.0(48.0)	-1.3(1.5)
$H_2\cdots X_{NN}$	-10.7	49.3	-33.2(55.4)	-25.4(42.4)	-1.3(2.2)
$2H_2\cdots X_{NN}$	-7.6	41.7	-26.6(53.9)	-21.4(43.4)	-1.3(2.7)
$3H_2\cdots X_{NN}$	-6.0	29.6	-18.5(51.9)	-15.1(42.3)	-2.0(5.7)
$4H_2\cdots$Ni-X_{NN}	-44.9	213.0	-144.2(55.9)	-108.5(42.1)	-5.1(2.0)
$8H_2\cdots$3Ni-X_{NN}	-30.2	164.0	-104.1(53.9)	-84.6(43.5)	-5.5(2.8)

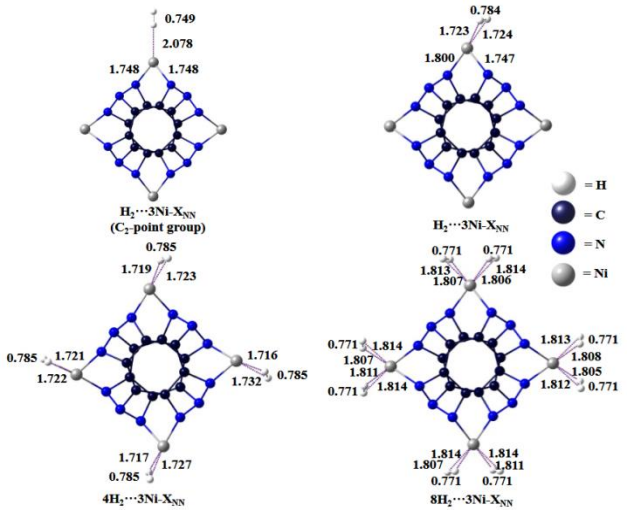

Fig. 4. Optimized structures of $nH_2\cdots$3Ni-X_{NN} (n=1, 4, 8) at the ωB97X-D/Def2-TZVP level.

The minimum energy H_2 loaded or relaxed structures of 3Ni-X_{NN} (having D_{2d} point group symmetry) on the potential energy surface (PES) are shown in **Fig. 4**. The single H_2 molecule adsorption on 3Ni-X_{NN} is found to align in two different ways, i) side-on orientation and ii) end-on orientation. In the case of side-on orientation, the H-H distance is elongated more than that in the latter and partial dissociation is observed therein. The adsorption free energy values for all the H_2 binding processes are negative which indicates that the adsorption processes are exergonic in nature and these processes are thermodynamically spontaneous except for the maximum H_2 loaded case, where slight cryogenic temperature is required when the unfavorable $T\Delta S$ term exceeds the favorable ΔH term giving positive value for ΔG_{ads} term. A

step-by-step flow diagram of the entire process, starting from $C_{12}N_{12}$ to $8H_2\cdots3Ni\text{-}X_{NN}$, is depicted in **Fig. 5** along with the corresponding values of formation energy.

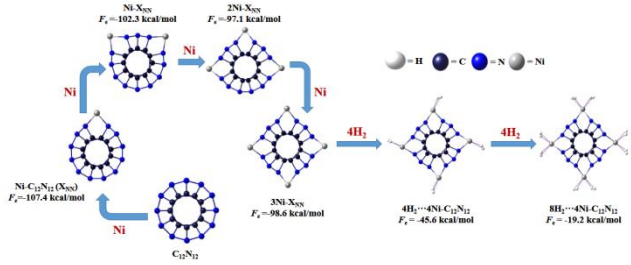

Fig. 5. Formation energies (E_e, kcal/mol) of the shown processes at the ωB97X-D/Def2-TZVP level.

Conclusion

Using DFT calculations, it has been observed that the systematic decoration of Ni in a different mode of bridging on $C_{12}N_{12}$ nano-cluster can tune the H_2 storage capacity. The calculated binding energy and free energy change of adsorption infer that the structures of Ni-$C_{12}N_{12}$ and $H_2\cdots$Ni-$C_{12}N_{12}$ are thermodynamically feasible. NPA charge calculation indicates that the polar nature of Ni-C or Ni-N bonds are responsible for H_2 interaction as well as their partial dissociation on adsorption. It has been found that a positively charged Ni atom on $C_{12}N_{12}$ can adsorb up to three H_2 molecules. The average adsorption energies of H_2 molecules have been found to be within the range (11.9-23.3 kcal/mol for C-(μ-Ni)-N bridge case versus 16.0-39.2 kcal/mol for the N-(μ-Ni)-N case). The organization of four Ni in N, N bridging mode gives a new thermodynamically stable geometry (D_{2d} point group) that is potent for H_2 storage as well. Aromaticity increases on Ni doping in a symmetric and systematic fashion surrounding the $C_{12}N_{12}$ cluster.

Acknowledgements

PKC would like to thank Dr. Pan Wang and Prof. Ashutosh Tiwari for kindly inviting him to contribute an article to the Advanced Materials Letters on the occasion of the 10th anniversary of the International Association of Advanced Materials, IAAM. He also thanks DST, New Delhi for the J. C. Bose National Fellowship. GJ and RP thank IIT, Kharagpur, and CSIR respectively, for their fellowships. SM thanks the University Grants Commission, New Delhi for UGCBSR Research Start-Up-Grant (No. F.30-458/2019(BSR)) for funding, and Centre for Theoretical Studies, IIT Kharagpur for the CTS Visitors' Program.

Conflicts of interest

The authors declare that they have no conflict of interests regarding the publication of this article, financial, and/or otherwise.

Keywords

Nickel decorated $C_{12}N_{12}$, structure and stability, isodesmic reaction, aromaticity, H_2 storage.

Received: 26 February 2020
Revised: 17 March 2020
Accepted: 17 March 2020

References

1. Schlapbach, L.; Züttel, A.; *Nature*, **2001**, *414*, 353.
2. Lubitz, W.; Tumas, W.; *Chem. Rev.*, **2007**, *107*, 3900.
3. Lewis, N.S.; Nocera, D.G.; *Proc. Natl. Acad. Sci.*, **2006**, *103*, 15729.
4. Coontz, R.; Hanson, B.; Not so simple; *American Association for the Advancement of Science*, **2004**, *305*, 957.
5. Züttel, A.; Wenger, P.; Sudan, P.; Mauron, P.; Orimo, S. I.; *Mat. Sci. Eng. B*, **2004**, *108*, 9.
6. Cohen, R. L.; Wernick, J.; *Science*, **1981**, *214*, 1081.
7. Graetz, J.; *Chem. Soc. Rev.*, **2009**, *38*, 73.
8. Deng, W.Q.; Xu, X.; Goddard, W. A.; *Phys. Rev. Lett.*, **2004**, *92*, 166103.
9. Froudakis, G. E.; *Nano Lett.*, **2001**, *1*, 179.
10. Heine, T.; Zhechkov, L.; Seifert, G.; *Phys. Chem. Chem. Phys.*, **2004**, *6*, 980.
11. Wu, X.; Gao, Y.; Zeng, X. C.; *J. Phys. Chem. C*, **2008**, *112*, 8458.
12. Jana, G.; Pal, R.; Chattaraj, P. K.; *J. Indian Chem. Soc.*, **2018**, *95*, 1457.
13. McKeown, N. B.; Gahnem, B.; Msayib, K. J.; Budd, P. M.; Tattershall, C. E.; Mahmood, K.; Tan, S.; Book, D.; Langmi, H. W.; Walton, A.; *Angew. Chem. Int. Ed.*, **2006,** *45*, 1804.
14. Lee, H.; Lee, J. W.; Kim, D. Y.; Park, J.; Seo, Y. T.; Zeng, H.; Moudrakovski, I. L.; Ratcliffe, C. I.; Ripmeester, J. A.; *Nature*, **2005**, *434*, 743.
15. Chattaraj, P. K.; Bandaru, S.; Mondal, S.; *J. Phys. Chem. A*, **2010**, *115*, 187.
16. Fraenkel, D.; Shabtai, J.; *J. Am. Chem. Soc.*, **1977**, *99*, 7074.
17. Langmi, H.; Walton, A.; Al-Mamouri, M.; Johnson, S.; Book, D.; Speight, J.; Edwards, P.; Gameson, I.; Anderson, P.; Harris, I.; *J. Alloy. Compd.*, **2003**, *356*, 710.
18. Langmi, H.; Book, D.; Walton, A.; Johnson, S.; Al-Mamouri, M.; Speight, J.; Edwards, P.; Harris, I.; Anderson, P.; *J. Alloy. Compd.*, **2005**, *404*, 637.
19. Vitillo, J. G.; Ricchiardi, G.; Spoto, G.; Zecchina, A.; *Phys. Chem. Chem. Phys.* **2005**, *7*, 3948.
20. Yanagisawa, T.; Shimizu, T.; Kuroda, K.; Kato, C.; *B. Chem. Soc. Jpn.*, **1990**, *63*, 988.
21. Beck, J. S.; Vartuli, J.; Roth, W. J.; Leonowicz, M.; Kresge, C.; Schmitt, K.; Chu, C.; Olson, D. H.; Sheppard, E.; McCullen, S.; *J. Am. Chem. Soc.*, **1992**, *114*, 10834.
22. Kresge, C.; Leonowicz, M.; Roth, W. J.; Vartuli, J.; Beck, J.; *Nature*, **1992**, *359*, 710.
23. Zhao, D.; Feng, J.; Huo, Q.; Melosh, N.; Fredrickson, G. H.; Chmelka, B. F.; Stucky, G. D.; *Science*, **1998**, *279*, 548.
24. Rosi, N. L.; Eckert, J.; Eddaoudi, M.; Vodak, D. T.; Kim, J.; O'Keeffe, M.; Yaghi, O. M.; *Science* **2003**, *300*, 1127.
25. Rowsell, J.L.; Yaghi, O.M.; *Angew. Chem. Int. Ed.*, **2005**, *44*, 4670.
26. Cabria, I.; López, M.; Alonso, J.; *Phys. Rev. B*, **2008**, *78*, 075415.
27. Kuc, A.; Zhechkov, L.; Patchkovskii, S.; Seifert, G.; Heine, T.; *Nano Lett.*, **2007**, *7*, 1.
28. Kabbour, H.; Baumann, T. F.; Satcher, J. H.; Saulnier, A.; Ahn, C. C.; *Chem. Mater.*, **2006**, *18*, 6085.
29. Tian, H.Y.; Buckley, C.; Wang, S.; Zhou, M.; *Carbon* **2009**, *47*, 2128.
30. Baldé, C. P.; Hereijgers, B. P.; Bitter, J. H.; de Jong, K. P.; *Angew. Chem. Int. Ed.*, **2006**, *45*, 3501.
31. Sun, Q.; Wang, Q.; Jena, P.; *Nano Lett.*, **2005**, *5*, 1273.
32. Jana, G.; Pan, S.; Rodríguez-Kessler, P. L.; Merino, G.; Chattaraj, P. K.; *J. Phys. Chem. C*, **2018**, *6*, 27941.
33. Kojima, Y.; Suzuki, K.-i.; Fukumoto, K.; Sasaki, M.; Yamamoto, T.; Kawai, Y.; Hayashi, H.; *Int. J. Hydrogen Energ.*, **2002**, *27*, 1029.
34. Wicke, E.; Brodowsky, H.; Züchner, H.; Hydrogen in Metals II, Application-Oriented Properties. Springer-Verlag, Berlin, **1978**.
35. Alefeld, G.; Völkl, J.; Hydrogen in metals I-Basic properties; Berlin and New York, Springer-Verlag, **1978**.
36. Sakintuna, B.; Lamari-Darkrim, F.; Hirscher, M.; *Int. J. Hydrogen Energ.*, **2007**, *32*, 1121.
37. Johnson, A.; Daley, S.; Utz, A.; Ceyer, S.; *Science*, **1992**, *257*, 223.
38. Johnson, A.; Maynard, K.; Daley, S.; Yang, Q.; Ceyer, S.; *Phys. Rev. Lett.*, **1991**, *67*, 927.
39. Maynard, K. J.; Johnson, A. D.; Daley, S. P.; Ceyer, S. T.; *Faraday Discuss. Chem. Soc.*, **1991**, *91*, 437.
40. Wilde, M.; Fukutani, K.; Ludwig, W.; Brandt, B.; Fischer, J. H.; Schauermann, S.; Freund, H.J.; *Angew. Chem. Int. Ed.*, **2008**, *47*, 9289.

41. Wilde, M.; Fukutani, K.; Naschitzki, M.; Freund, H. J.; *Phys. Rev. B* **2008**, *77*, 113412.
42. Jiang, D.; Carter, E. A.; *Surf. Sci.*, **2003**, *547*, 85.
43. Xu, L.; Xiao, H.; Zu, X.; *Chem. Phys.*, **2005**, *315*, 155.
44. Greeley, J.; Krekelberg, W. P.; Mavrikakis, M.; *Angew. Chem. Int. Ed.*, **2004**, *43*, 4296.
45. Panczyk, T.; Rudzinski, W.; *Appl. Surf. Sci.*, **2004**, *233*, 141-154.
46. Kalamse, V.; Wadnerkar, N.; Deshmukh, A.; Chaudhari, A.; *Int. J. Hydrogen Energ.*, **2012**, *37*, 5114.
47. Gudmundsdóttir, S.; Skúlason, E.; Jónsson, H.; *Phys. Rev. Lett.*, **2012**, *108*, 156101.
48. Greeley, J.; Mavrikakis, M.; *J Phys. Chem. B*, **2005**, *109*, 3460.
49. Ferrin, P.; Kandoi, S.; Nilekar, A. U.; Mavrikakis, M.; *Surf. Sci.*, **2012**, *606*, 679.
50. Yarovsky, I.; Goldberg, A.; *Mol. Simulat.*, **2005**, *31*, 475.
51. Jagiello, J.; Ansón, A.; Martínez, M. T.; *J. Phys. Chem. B*, **2006**, *110*, 4531.
52. Guo, L.; Wu, H. S.; Jin, Z. H.; *Appl. Surf. Sci.*, **2005**, *242*, 88.
53. Wang, Q.; Sun, Q.; Jena, P.; Kawazoe, Y.; *ACS nano*, **2009**, *3*, 621.
54. Rad, A. S.; Abedini, E.; *Appl. Surf. Sci.*, **2016**, *360*, 1041.
55. Rad, A. S.; *Synth. Met.*, **2016**, *211*, 115.
56. Rad, A. S.; Jouibary, Y. M.; Foukolaei, V. P.; Binaeian, E.; *Curr. Appl. Phys.* **2016**, *16*, 527.
57. Rad, A. S.; Shabestari, S. S.; Mohseni, S.; Aghouzi, S. A. *J. Solid State Chem.*, **2016**, *237*, 204.
58. Rad, A. S.; Foukolaei, V. P.; *Synth. Met.*, **2015**, *210*, 171.
59. Rad, A. S.; *Surf. Sci.*, **2016**, *645*, 6.
60. Rad, A. S.; Ayub, K.; *J. Alloy.Compd.* **2016**, *678*, 317.
61. Shevlin, S.; Guo, Z.; *Appl. Phys. Lett.*, **2006**, *89*, 153104.
62. Giri, S.; Chakraborty, A.; Chattaraj, P. K.; *Nano Revi.*, **2011**, *2*, 5767.
63. Xu, W.J.; Hu, Z.Y.; Shao, X.H.; *Acta Phys-Chim. Sin.*, **2012**, *28*, 1721.
64. Rad, A. S.; Ayub, K.; *Int. J. Hydrogen Energ.*, **2016**, *41*, 22182.
65. Schleyer, P. V. R.; Wuerthwein, E. U.; Pople, J. A.; *J. Am. Chem. Soc.*, **1982**, *104*, 5839..
66. Schleyer, P. V. R.; Wuerthwein, E. U.; Kaufmann, E.; Clark, T.; Pople, J. A.; *J. Am. Chem. Soc.*, **1983**, *105*, 5930.
67. Wu, C.; Kudoa, H.; Ihle, H.; *J. Chem. Phys.*, **1979**, *70*, 1815.
68. Kudo, H.; *Nature*, **1992**, *355*, 432.
69. Mondal, S.; Srinivasu, K.; Ghosh, S. K.; Chattaraj P. K.; *Rsc. Adv.* **2013**, 3, 6991.
70. Hofmann, A. W. V.; *Proc. R. Soc. Lond.*, **1857**, 8, 1.
71. von Ragué Schleyer, P.; *Chem. Rev.*, **2001**, *5*, 1115.
72. Cyvin, S. J.; Gutman, I.; Kekulé structures in benzenoid hydrocarbons; Springer-Verlag, Berlin Heidelberg, **2013**.
73. Minkin, V. I.; Glukhovtsev, M. N.; Simkin, B. Y.; Aromaticity and antiaromaticity; J. Wiley & Sons, NY, **1994**.
74. Balaban, A. T.; Oniciu, D. C.; Katritzky, A. R.; *Chem. Rev.*, **2004**, *104*, 2777.
75. Ashe III, A. J.; *J. Am. Chem. Soc.*, **1971**, *93*, 3293.
76. Elliott, G. P.; Roper, W. R.; Waters, J. M.; *J. Chem. Soc. Chem. Commun.*, **1982**, 811.
77. Li, X.; Kuznetsov, A. E.; Zhang, H. F.; Boldyrev, A. I.; Wang, L. S.; *Science*, **2001**, *291*, 859.
78. Chen, Z.; Wannere, C. S.; Corminboeuf, C.; Puchta, R.; Schleyer, P. V. R.; *Chem. Rev.* **2005**, *105*, 3842.
79. Kealy, T.; Pauson, P.; *Nature*, **1951**, *168*, 1039.
80. Wilkinson, G.; Rosenblum, M.; Whiting, M.; Woodward, R.; *J. Am. Chem. Soc.*, **1952**, *74*, 2125.
81. Eiland, P. F.; Pepinsky, R.; *J. Am. Chem. Soc.*, **1952**, *74*, 4971.
82. Coriani, S.; Haaland, A.; Helgaker, T.; Jørgensen, P.; *Chem. Phys. Chem.*, **2006**, *7*, 245.
83. Kudinov, A.; Rybinskaya, M.; *Russ. Chem. Bull.*, **1999**, *48*, 1615.
84. Kudinov, A. R.; Loginov, D. A.; Starikova, Z. A.; Petrovskii, P. V.; *J. Org. Chem.*, **2002**, *649*, 136.
85. Beck, V.; O'Hare, D.; *J. Org. Chem.*, **2004**, *689*, 3920.
86. Qian-shu, L.; Heng-tai, Y.; Au-chin, T.; *Theor. Chim. Acta.*, **1986**, *70*, 379..
87. Malar, E. P.; *Theor. Chem. Acc.* **2005**, *114*, 213.
88. Kruszewski, J.; Krygowski, T.; *Tetrahedron Lett.*, **1972**, *13*, 3839.
89. Krygowski, T. M.; *J. Chem. Inf. Comput. Sci.*, **1993**, *33*, 70.
90. Pauling, L.; Sherman, J.; *J. Chem. Phys.* **1933**, *1*, 606.
91. Hehre, W. J.; Ditchfield, R.; Radom, L.; Pople, J. A.; *J. Am. Chem. Soc.*, **1970**, *92*, 4796.
92. Schleyer, P. V. R.; Pühlhofer, F.; *Org. Lett.*, **2002**, *4*, 2873.
93. Julg, A.; François, P.; *Theor. Chim. Acta.*, **1967**, *8*, 249.
94. Bergmann, E. D.; Pullman, B.; In Aromaticity, pseudo-aromaticity, anti-aromaticity, Israel Academy of Sciences & Humanities: **1971**.
95. Krygowski, T.M.; Szatylowicz, H.; Stasyuk, O.A.; Dominikowska, J.; Palusiak, M.; *Chem. Rev.*, **2014**, *114*, 6383.
96. Jug, K.; Köster, A. M.; *J. Phys. Org. Chem.* **1991**, *4*, 163.
97. Matito, E.; Duran, M.; Sola, M.; *J. Chem. Phys.*, **2005**, *122*, 014109.
98. Bird, C. W.; *Tetrahedron* **1986**, *42*, 89.
99. Bird, C. W.; *Tetrahedron* **1992**, *48*, 335.
100. Bird, C. W.; *Tetrahedron* **1996**, *52*, 9945.
101. Sundholm, D.; Fliegl, H.; Berger, R. J.; *Wiley Interdisciplinary Reviews: Comp. Mol. Sci.*, **2016**, *6*, 639.
102. Giambiagi, M.; de Giambiagi, M. S.; dos Santos Silva, C. D.; de Figueiredo, A. P.; *Phys. Chem. Chem. Phys.*, **2000**, *2*, 3381.
103. Howard, S.; Krygowski, T.; *Can. J. Chem.*, **1997**, *75*, 1174.
104. Matta, C. F.; Hernández-Trujillo, J.; *J. Phys. Chem. A*, **2003**, *107*, 7496.
105. Mandado, M.; González-Moa, M. J.; Mosquera, R. A.; *J. Comput. Chem.*, **2007**, *28*, 127.
106. Poater, J.; Fradera, X.; Duran, M.; Sola, M.; *Chem. Eur. J.*, **2003**, *9*, 400.
107. Juse, J.; Sundholm, D.;. *Phys. Chem. Chem. Phys.*, **1999**, *1*, 3429.
108. Imoto, H.; Fujii, T.; Tanaka, S.; Yamamoto, S.; Mitsuishi, M.; Yumura, T.; Naka, K.; *Org. Lett.*, **2018**, *20*, 5952.
109. Herges, R.; Geuenich, D.; *J. Phys. Chem. A*, **2001**, *105*, 3214.
110. Schleyer, P. V. R.; Maerker, C.; Dransfeld, A.; Jiao, H.; van Eikema Hommes, N. J.; *J. Am. Chem. Soc.*, **1996**, *118*, 6317.
111. Solà i Puig, M.; *Front. Chem.*, **2017**, *5*, 22.
112. Moran, D.; Stahl, F.; Bettinger, H. F.; Schaefer, H. F.; Schleyer, P. V. R. *J. Am. Chem. Soc.*, **2003**, *125*, 6746.
113. Ruiz-Morales, Y.; *J. Phys. Chem. A*, **2004**, *108*, 10873.
114. Li, X. W.; Pennington, W. T.; Robinson, G. H.; *J. Am. Chem. Soc.*, **1995**, *117*, 7578.
115. Xie, Y.; Schreiner, P. R.; Schaefer, H. F.; Li, X. W.; Robinson, G. H.; *J. Am. Chem. Soc.*, **1996**, *118*, 10635.
116. Nyulászi, L.; *Chem. Revi.*, **2001**, *101*, 1229.
117. Chai, J. D.; Head-Gordon, M.; *Phys. Chem. Chem. Phys.*, **2008**, *10*, 6615.
118. Grimme, S.; *J. Comput. Chem.*, **2006**, *27*, 1787.
119. Weigend, F.; Ahlrichs, R.; *J. Am. Chem. Soc.*, **2005**, *7*, 3297.
120. Weigend, F.; *J. Am. Chem. Soc.*, **2006**, *8*, 1057.
121. Frisch, M. J.; Trucks, G. W.; Schlegel, H. B.; Scuseria, G. E.; Robb, M. A.; Cheeseman, J. R.; et al., Gaussian 09, Revision C.01, Wallingford CT: Gaussian, Inc.; **2010**.
122. Reed, A. E.; Weinhold, F.; *J. Chem. Phys.*, **1983**, *78*, 4066.
123. Glendening, E. D.; Landis, C. R.; Weinhold, F.; *J. Comput. Chem.*, **2013**, *34*, 1429.
124. Krim, J.; *Am. J. Phys.*, **2002**, 70, 890.
125. Grimme, S.; Antony, J.; Ehrlich, S.; Krieg, H.; *J. Chem. Phys.*, **2010**, *132*, 154104.
126. Te Velde, G. T.; Bickelhaupt, F. M.; Baerends, E. J.; Fonseca Guerra, C.; van Gisbergen, S. J.; Snijders, J. G.; Ziegler, T.; *J. Comput. Chem.*, **2001**, *22*, 931.
127. Baerends, E. J.; Ziegler, T.; Autschbach, J.; Bashford, D.; Bérces, A.; Bickelhaupt, F.; Bo, C.; Boerrigter, P.; Cavallo, L.; Chong, D., ADF2013, SCM, Theoretical Chemistry, Vrije Universiteit, Amsterdam, The Netherlands. **2014**.
128. Wolff, S.; Ziegler, T.; Van Lenthe, E.; Baerends, E.; *J. Chem. Phys.*, **1999**, *110*, 7689.
129. Chase, M.; Davies, C.; Downey, J.; Frurip, D.; McDonald, R., *J. Phys. Chem. Ref. Data. JANAF Thermochemical Tables*, New York, **1998**.
130. Scott, D. W.; Berg, W. T.; Hossenlopp, I.; Hubbard, W. N.; Messerly, J. F.; Todd, S. S.; Douslin, D. R.; McCullough, J. P.; Waddington, G.; *J. Phys. Chem.*, **1967**, *71*, 2263.

Authors Biography

Gourhari Jana is a 5th-year research scholar working under Professor Pratim Kumar Chattaraj, Department of Chemistry, Indian Institute of Technology Kharagpur. He has already co-authored 30 journal articles including one book chapter. His research activities include electronic structure theory, machine learning and deep learning, QSAR/QSPR/QSTR analyses, quantum trajectory (ADMP, BOMD), Time-Dependent Density Functional Theory (TDDFT), Non-Linear Optical (NLO) properties, Adaptive Natural Density Partitioning (AdNDP) method, aromaticity, etc. in the domain of theoretical and computational chemistry.

Ranita Pal is a 2nd year research scholar at Centre for Theoretical Studies, Indian Institute of Technology Kharagpur working under Professor Pratim Kumar Chattaraj. She has already co-authored 4 journal articles and a book chapter. Her research activities include electronic structure theory, hydrogen storage, chemical reactivity, binding of small molecules and isomerization processes, studies on Adaptive Natural Density Partitioning method (AdNDP, investigation of nc-2e bond), machine learning and QSAR/QSPR/QSTR analyses in the domain of theoretical and computational chemistry.

Sukanta Mondal is an Assistant Professor in Chemistry at Department of Education, Assam University, Silchar. He completed his Ph.D. in 2015 under the guidance of Prof. Pratim Kumar Chattaraj from Department of Chemistry, IIT Kharagpur. His research interests include classical and quantum simulations, DFT calculations and dispersion corrected DFT calculations. He was a National Postdoctoral Fellow, SERB, India at JNCASR, Bengaluru. Recently he has received the UGC-BSR Research Start-Up grant from UGC, India.

Pratim Kumar Chattaraj is an Institute Chair Professor at the Indian Institute of Technology Kharagpur. His research interests include density functional theory, nonlinear dynamics, aromaticity in metal clusters, hydrogen storage, noble gas compounds, machine learning, chemical reactivity and quantum trajectories. He is a Fellow of The World Academy of Sciences and all three Indian Science Academics He is a Sir J.C. Bose National Fellow. Several of his papers have become Editors' choice/hot/most cited/most accessed/cover articles.

Graphical Abstract

Ni-decorated polycyanogen clusters, $C_{12}N_{12}$, exhibiting three different isomeric forms, are promising high-energy-density materials for Hydrogen storage. Gas-phase heat of formation suggests the spontaneous formation of the Ni-decorated $C_{12}N_{12}$ cluster. Systematic Ni decoration enhances the aromaticity of the $C_{12}N_{12}$ cluster. Interaction energy between H_2 and Ni-decorated $C_{12}N_{12}$ cluster mainly originates from the electrostatic and orbital interactions.